Title

EFFECT OF LASER HARDENING ON MICROSTRUCTURE AND WEAR RESISTANCE IN MEDIUM CARBON/CHROMIUM STEELS

Authors

Kusinski, J.
Thomas, G.

Publication Date

1986-04-01

Lawrence Berkeley Laboratory
UNIVERSITY OF CALIFORNIA

Materials & Molecular Research Division

To be presented at the Symposium on Optical and Optoelectronic Applied Sciences and Engineering, Quebec, Canada, June 2-6, 1986

EFFECT OF LASER HARDENING ON MICROSTRUCTURE AND WEAR RESISTANCE IN MEDIUM CARBON/CHROMIUM STEELS

J. Kusinski and G. Thomas

April 1986

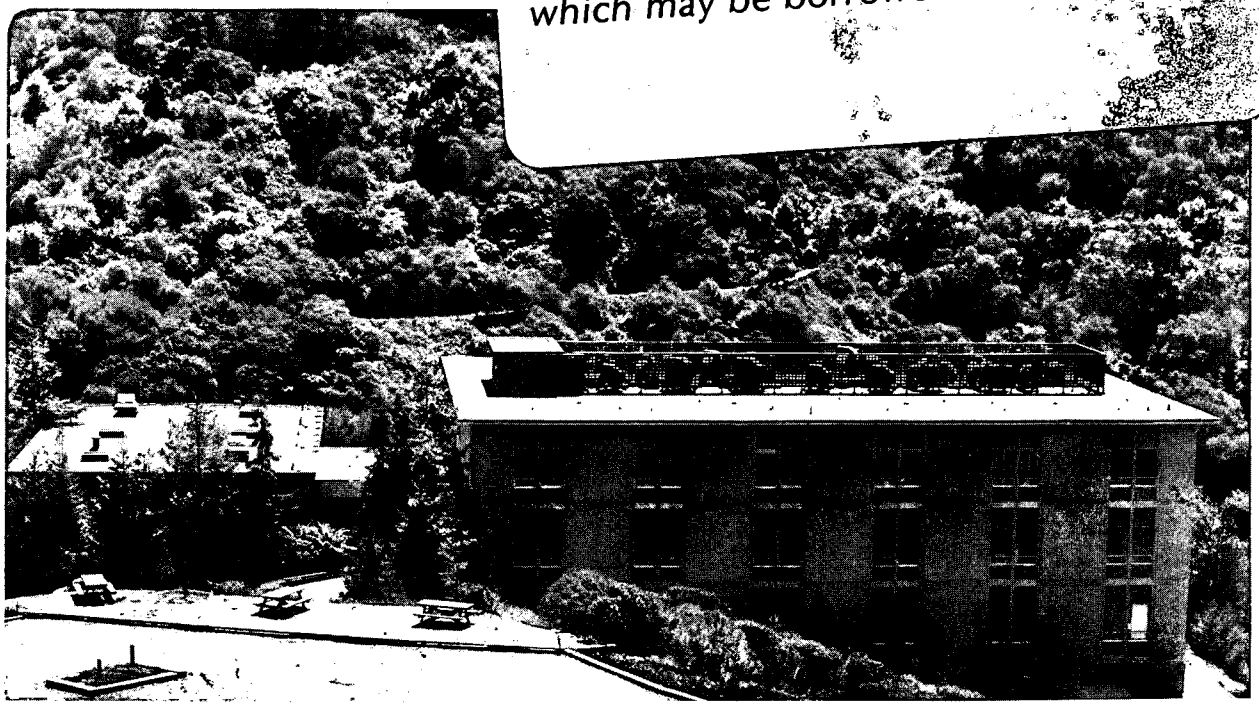

Prepared for the U.S. Department of Energy under Contract DE-AC03-76SF00098

DISCLAIMER

EFFECT OF LASER HARDENING ON MICROSTRUCTURE AND WEAR RESISTANCE IN MEDIUM CARBON/CHROMIUM STEELS

Jan Kusinski* and Gareth Thomas

Department of Materials Science and Mineral Engineering, and National Center for Electron Microscopy, Materials and Molecular Research Division, Lawrence Berkeley Laboratory, University of California, Berkeley, CA 94720, U.S.A.
*Visiting Scientist, Institute of Metallurgy, University of Mining and Metallurgy, 30059 Cracow, Poland.

Abstract

Metallographical (optical, TEM, SEM), spectroscopic, abrasive wear resistance and microhardness investigations of Fe/Cr/Mn/C steels heat-treated by a continuous CO_2 laser are described. Laser hardening resulted in wear resistance of 1.4 - 1.6 times better than that of conventionally hardened steels. Laser melting followed by rapid solidification allows formation of a solidified layer with high wear resistance only when the scanning velocity and mass of the samples were sufficient to realize high cooling rates. The variations in the wear resistance and microhardness with distance from the heated surface were similar. The grain refinement caused by rapid laser-heating and high stresses induced during cooling create essentially fine, highly dislocated lath and internally twinned martensites with some amount of stable, interlath retained austenite. This structure has in turn beneficial effects on wear resistance, and toughness. Laser-heat treatment for deep melting of the surface layers of the steels shows only a small improvement in wear resistance. Such heat-treatment results in delta ferrite retention (10Cr steel) and chromium segregation to cell-boundaries.

Introduction

The Fe/Cr/Mn/C steels have been developed for superior combinations of strength, toughness and both sliding and abrasive wear resistance.[1] Thomas et al.[2,3] showed that improvements in toughness, with little or no change in strength may be realized in medium-carbon steels by appropriate design of composite microstructures of fine grained martensite surrounded by stable retained austenite films. Highly dislocated lath martensite with continuous films of retained austenite appears to be a preferable microstructure for good sliding and abrasive wear resistance.[4,5] Grain refining was found to increase the volume fraction of retained austenite.[6] Some of these factors (grain size, stability of austenite, substructure of martensite) and consequently mechanical properties and abrasive resistance can be enhanced by rapid heating and cooling processes, for instance electron or laser-beam heating. Extremely rapid heating and cooling rates inherent in laser heating makes hardening of steels possible and relatively easy. Recent applications of lasers to materials processing include surface melting, alloying, cladding, heat-treating, and shock hardening.[7] The present status of the various aspects of laser-heating processes can be found in a number of conference proceedings,[7,8] review papers,[9,10] and books.[11,12] A review of the literature shows that, while significant advances have been made recently in the theory of laser heating of solids,[13] rapid solidification after laser melting,[9,14] cutting and welding of alloys,[15] properties of steels and cast-iron after laser-surface-heating or melting,[9,11] a detailed understanding of the basic phenomena of laser hardening remains to be obtained. Several researches have already studied wear resistance of steels after laser heat-treatment.[7,18,19,20] Kikuchi et al. reported that wear resistance of laser heat-treated JISSK5 steel is twice as good as that of induction hardened material due to the presence of highly deformed martensite formed during laser heat-treatment (LHT) under unusually high restraints.[18] According to Gnanamuthu the wear resistance of AISI 1045 steel after LHT is higher than that of conventionally heat-treated.[19] Preliminary studies by Rayment and Thomas of wear resistance of LHT experimental Fe/3Cr/0.3C steel indicate a substantial increase in sliding wear resistance as compared to that of samples after conventional heat-treatment.[20] They concluded that high residual compressive stresses in the surface-treated layer appear to contribute to the hardness and hence to the sliding wear resistance. Thus based on past research, the following benefits can be anticipated from laser-hardening:

- The residual compressive stresses developed at the laser-treated layer due to martensitic transformation improve fatigue, hardness, abrasive and erosive wear, and corrosive resistance.
- Higher hardness and strength of steels, compared to that observed after conventional heat-treatment, can be achieved without necessarily losing toughness.
- The grain refinement and increased chemical homogeneity of steels resulting from rapid solidification (if melting occurs) can be expected to create beneficial effects on mechanical properties and corrosive resistance.

The reason for these benefits are not only the extreme rates of heating and cooling of the material (which cause unusually high restraints), but also frequently the high pressure, which involves deformation of the materials (i.e., laser-shocking[16]). Subsequent rapid cooling after heating has a notable influence on the solidification, phase transformations and also on precipitation processes. The current study of 3Cr and 10Cr steels, heated through both conventional and laser heat-treating processes has been directed at determining the abrasive wear resistance, hardness and microstructure as a function of different heat-treatments.

Experimental Procedure

Experimental work was carried out on two types of chromium steel Fe/3.11Cr/1.98Mn/0.5Mo/0.26C-(3Cr) and Fe/9.85Cr/1.0Mn/0.5Al/0.20C -(10Cr) previously developed in the alloy design program.[2] The alloys used in this investigation were supplied by Diado Steel Company, Japan (3Cr), and by Allegheny Ludlum Steel Corporation, USA (10Cr). They were vacuum induction melted, casted into 9kg ingots and subsequently rolled to 2.5 cm thick and 62.5 cm wide plates and homogenized under argon atmosphere at 1200°C for 24 hours. 9cm x 7cm x 2cm plates were cut from such prepared materials. Some of plates were cut into 9cm x 2cm x 2cm rectangular pieces, lathe machined to 9cm long by 1.5cm diameter rods and hot-rolled to 6.25mm dia. rods. Rolled rods were lathe-machined to 6mm dia. and cut into 20mm long pins. Prior to laser heat-treatment plates and pins were conventionally heat-treated (CHT) to have the microstructure found previously to assure the optimum combination of mechanical properties.[2,3] They were austenitized at 1100°C for 1hr, oil quenched, 200°C tempered for 1hr and then re-austenitized at 870°C for 1hr and oil quenched. Austenitization was done under an argon atmosphere. After that samples were surface ground and abraded on 320 silicon-carbide paper.

The laser heat-treatment (LHT) was carried out at Coherent Laser Inc. of Palo Alto using an EFA-51 1250kW CO_2 laser with cylindrical lens producing an narrow-elliptical spot (see Figure 1). The scheme of LHT is presented in Figure 2. LHT was done under a helium protective atmosphere. The sample-surfaces were scanned by the beam at velocites 25.4cm/min (LHT1), 38cm/min (LHT2), and 50.8cm/min (LHT3). Such a LHT produced melted (after LHT1 and LHT2) or only heat-treated (after LHT3) surface-layers. After LHT some samples were tempered at 200°C, 350°C, and 500°C for 2 hours. Wear testing was performed using two-body (pin-on-disc), dry abrasive wear system. The wear pins were worn against abrasive paper (120 SiC grit) for 10 revolutions at a rotation speed of 20rpm under 1 and 2kg dead-weight loads. The specimens were weighed before and after each test using an electronic Mettler AE163 analytical balance to an accuracy of 0.01mg. The weight loss was than determined and converted to wear resistance (W_r) using the relation:

$$W_r = \frac{\text{material density x length of wear path}}{\text{weight loss}} \text{ mm/mm}^3 \qquad (1)$$

In addition to the 3Cr and 10Cr samples some of the AISI 1018 samples were also tested for comparison of the present results with that obtained for conventionally heat-treated steels in previous investigations.[4,5] For comparison a relative wear resistance coefficient R_{wr} was calculated as:

$$R_{wr} = \frac{W_{ri}}{W_{r1018}} = \frac{\text{wear resistance of "i" sample}}{\text{wear resistance of 1018 steel}} \qquad (2)$$

Optical metallography (OM), scanning(SEM) and transmission electron microscopy (TEM) and energy dispersive x-ray (EDX) analysis have been used to characterize the structure of the solidified and the solid-state-transformed zones. Specimens for OM examination were cut from LHT plates and worn pins. Cross-sections were made in all three perpendicullar planes. Samples were polished mechanically. An electrolytical etching in 6% aqueous solution of CrO_3 at 8V was used to reveal the microstructure of laser-melted zones. The martensitic microstructure was resolved after etching in Villella's (10Cr) and 5% nital (3Cr) reagents. In addition to metallography, the Rockwell hardness and the microhardness using a Micromet miniload hardness tester with a Knoop diamond indenter (100g load) were determined. TEM examinations were carried out on thin foil specimens obtained from 0.5mm slices cut parallel and perpendicular to the heated surface, and carefully polished down to about 0.05mm. 3mm discs were punched from these slices and chemically thinned to about 0.04mm. Discs were electropolished in a twin jet electropolishing apparatus at room temperature in a chromic-acetic solution at 45-50V and 30-40mA. TEM observations, diffraction, and microanalysis were done on Philips EM 301 and 400 microscopes operated at 100kV. Fractography was conducted on samples fractured at liquid nitrogen using AMR 1000 and ISI 130 scanning electron microscopes.

Results and Discussion

The optical micrographs in Figures 3,4,6,8 and 9 show changes in microstructure of the laser heated material with different scanning velocites. Schematically these structures are given in Figure 2. Surface-layers obtained during LHT1 and LHT2 heating show three marked zones: (i)-deep or shallow melted (DMZ or SMZ) - material heated above the solidus, (ii)-hardened zone (HAZ)-material heated to the austenitizing range, and (iii)-tempered zone (TZ)- material heated below the austenitizing range. Layers formed during LHT3 contain two zones: (i)-hardened (HZ) and tempered (TZ). In both cases of laser melting (SMZ and DMZ), it is clear that melting has produced a marked refinement in the scale of the dendritic microstructure, corresponding to the cooling rate. Moreover, there is a strong tendency for epitaxial growth on the substrate and an effect of "shape memory" to the primary grains (see Figure 5). The martensitic laths have frequently the same orientation in both the resolidified and un-melted parts of the grains. This indicates that the newly solidified crystals that grow epitaxially from the unmelted parts of grains have the same crystallographic orientation. The grains formed in the melted zone are very large, but they have the substructure of the fine cellular grains that determine martensite packet size in this zone (see Figures 5, 10a, b and 11a). The grain size of HAZ (below MZ) depends on the austenitization temperature reached during heating (see Figure 8). The region just below MZ is where the highest temperature was reached and this has characteristic, coarse and irregular grains. The grains in the central region of HAZ have a very fine (of about 8-10μm dia.), irregular nature. The internal structure of these grains is a very fine martensite. In the lower region of this zone some

undissolved carbides were observed due to a low austenitizing temperature and short time of heating. TEM and SEM investigations (see Figures 10 a,b and 11a) show the structure of the as-melted zone as cellular, consisting of ultrafine, internally twinned martensite surrounded by retained austenite films. The large, primary forming martensite plates were able to cross several cellular crystals (see Figures 10a, b). The cell boundaries do not stop martensite-growth and are sites for martensitic nucleation. Since, in the usual definition of a cellular solidification structure, the cells within a single grain all have the same crystallographic orientation and therefore cannot be separated by high-angle boundaries martensite plates growth through a few cells was possible. EDX analysis indicated a higher chromium concentration at the cell-boundaries compared to the cell-centers (see Figure 14). Delta ferrite was presented after LHT1 only in the 10Cr steel, at the boundary between the melted and HAZ (see Figure 16) at the edge of the melted pool (showed by Chan et al. as an area with maximum cooling rate[17]). The presence of o-ferrite in the 10Cr steel may be expected because of the extended phase field compared to 3Cr steel (see equilibrium diagrams in Figure 7). Also, since the austenite phase field in the 3Cr steel is much wider than that of the 10Cr steel, it is easier to homogenise austenite during LHT of the 3Cr steel. No significant differences were observed between the microstructures of the laser-heated (after LHT3) and heat-affected zones of these two steels. A fine austenite grain-size also means a fine martensite packet microstructure and hence increases the amount of retained austenite films. The martensitic laths are ultrafine, dislocated with internal microtwinning and surrounded by the retained austenite films (see Figures 10 c-f and 14). Analysis of SAD patterns revealed a predominantly Kurdjumov-Sachs orientation relationship between austenite and martensite. In the top area of the hardened and HAZs some large martensitic laths, frequently containing autotempered epsilon carbide also were observed. The refining of the microstructure by laser heating is very well shown by SEM images of an overetched 3Cr steel in Figures 11 a, b and by fractographic results from the 10Cr steel in Figure 12.

Variations in the R_{wr} and microhardness as a function of scanning velocity, tempering temperature and depth from the heated surface are shown in Figures 16 a-c. Dot-dashed lines represent values of conventionally heat-treated samples. The values of R_{wr} of samples after LHT3 are the highest. With increasing tempering temperature, R_{wr} decrease (see Figure 16c). The softening of the 3Cr steel after LHT1 and LHT2 with tempering temperature and loss of good abrasive wear resistance is faster than that of 10Cr steel. R_{wr} obtained for samples after LHT3 are about 1.4-1.6 times better than that for CHT samples. The microhardness of LHT layers for 3Cr steel is about 600-650μHV_{100} units, and that for the 10Cr steel is about 600-700μHV_{100} units. Generally the microhardness and R_{wr} after LHT3 are higher and more uniform compared to that for LHT1 and LHT2. The distribution of microhardness in resolidified layers (after LHT1 and LHT2) is non uniform. This is caused by non homogeneous structure in that area. The lower level of microhardness near the melted surface can be explained as a result of local decarburization and oxidation processes during melting. Even in heated samples which were protected by a helium atmosphere a thin layer of surface oxides (Al and Cr) was observed. The second stage of microhardness and R_{wr} decrease was observed at the boundary between the melted and HAZs and correlated with both grain coarsening and the presence of δ-ferrite. The third stage was observed in the tempered zone. Although these local decreases in hardness and R_{wr} were discovered the mean values in the 500um thick laser-heated layer are higher than that for conventionally hardened steels (see Figures 16 c,d). Since variations in microhardness and R_{wr} are similar it seems that the hardness is the most dominant factor that determines abrasive resistance of these materials. This was also found earlier by Kwok and Thomas for conventionally hardened steels.[5] On the other hand the improvement in R_{wr} (1.4-1.6) is higher than that in hardness (1.1-1.3). This indicates that the toughness is improved after LHT and this may be important for higher abrasive resistance. Hornbogen[23] and Zum Gahr[24] have developed models that focus on the question of the threshold condition at which both plastic deformation and fracture are operating during wear. Although their models differ in detail it can be anticipated that the combination of the elastic modulus, hardness, fracture toughness and the frictional conditions in the contact area of the counterparts all play role in the abrasive wear rate of heat-treated steels.

Thus it is concluded that significant improvements in abrasive resistance are associated with increases of hardness, toughness and compressive stresses in the surface- layers due to the laser heat-treatment. The improvement in hardness can be explained by the ultrafine, highly dislocated and internally twinned martensite. The enhancement of toughness may be due to the grain refinement and increased continuity of the surrounding stable austenite films. Molian recently studied the effect of LHT on the microstructure and hardness of Fe-0.2C-Cr steels (produced from Fe-0.2C steel through laser surface-alloying process) and obtained similar microstructures irrespective of composition and cooling rate.[21] Thomas et al. showed that Fe/Cr/Mn/C steels improved strength and toughness by grain-refining treatments.[2,3,6] This is now shown to be very easily done by LHT, but the final results depend on initial structure of the steel and the rates of heating and cooling. Martensite produced from such rapid thermal processing of austenite by LHT has a finer structure with many lattice defects and higher hardness than martensite produced conventionally.[22] Residual compressive stresses develop at the laser hardened zone due to the volume increase (~3%) associated with the martensitic transformation. Although this investigation has not experimentally determined the toughness in the LHT condition it can be assumed that such microstructures would have good toughness, by mechanisms such as increased plasticity and crack stopping structures.[2] Hence these results show laser heat-treatment to be a promising method of heat-treating of medium carbon chromium steels when high hardness and wear resistance of the surface layer are required.

Summary

The main results obtained are as follows:

1. Laser heating with 50.8cm/min velocity results in a hardened layer of material with higher wear resistance

(1.4-1.6 times better) than that for conventionally hardened steels.
2. Both the melted and heat affected zones have higher hardness and R_{wr} than the substrate.
3. Since the improvement in R_{wr} is higher than that of hardness, toughness and compressive stresses are also factors that determine abrasive wear resistance of these steels.
4. The microstructures produced were essentially packet martensite (dislocated and fine twinned laths surrounded by retained austenite films).
5. The austenite-grain refinement caused by rapid laser-heating and high stresses induced during cooling create a refined packet structure of laths and retained austenite films.

Acknowledgements

The authors would like to acknowledge C.K. Kwok and T. Bielicki for their help during this investigation. Special thanks are due to Coherent Laser Inc.of Palo Alto for laser heat-treatment of the steels. This work was supported by the Director, Office of Energy Research, Office of Basic Energy Sciences, Materials and Molecular Sciences Division of the U.S. Department of Energy under Contract No. DE-AC03-76SF00098.

References

1. Pickering, F. B., Physical Metallurgy and Design of Steels, Applied Science Publishers LTD,London,p.127, 1978.
2. Thomas, G., Int. Conf. on Recent Dev. in Specialty Steels and Hard Materials, Pretoria, South Africa, Nov.,p.55, 1982.
3. Sarikaya, M., Steinberg, B. G., and Thomas, G., Met. Trans.A, Vol.13A, p.2227,1982.
4. Salesky, W. J., et al., Proc. Int. Conf. on Wear of Materials, Reston-Virginia, ASME, New York, p.434, 1983.
5. Kwok, C. K. and Thomas, G., Proc. Int. Conf. on Wear of Materials, Reston-Virginia, ASME, New York, p.140, 1983.
6. Narasimha Rao, B. V. and Thomas, G., Met. Trans.A, Vol.11A, p.441, 1980.
7. Metzbower, E. A., Conf. Proc. on Application of Lasers in Materials Processing, ASM, Metals Park, Ohio 1979.
8. Schuocker, D., Industrial Applications of High Power Lasers, SPIE, Linz, Austria, 1983.
9. Mazumder, J., J. of Metals, 35, 5, p.18, 1983.
10. Abil°siitov, G. A. and Velikov, E. A., Optics and Laser Technology, 2, p.30, 1984.
11. Metzbower, E. A., Source Book on Application of the Laser in Metalworking, ASM, Ohio, 1981.
12. Ready, J. F., Industrial Application of Lasers, New York, Academic Press, 1978.
13. Sparks, M., J. Appl. Physics, Vol.47, 3, p.837, 1976.
14. Mehrabian, R., Int. Met. Rev., Vol.27, 4, p.16, 1982.
15. Mazumder, J., J. of Metals, Vol.34, 7, p.16, 1982.
16. Clauer, A. H., et al., Met. Trans.A, Vol.8A, 12, p.1871, 1977.
17. Chan, C., et al., Met. Trans.A, Vol.15A, p.2175, 1984.
18. Kikuchi, M., et al., Proc. 1st Joint U.S./Japan Int. Laser Conf, Laser Institut of America, Toledo, Ohio, 1981.
19. Gnanamuthu, D. S., Proc. of Conf. on Appl. of Lasers in Materials Processing, ASM, Metals Park, Ohio, p.177, 1979.
20. Rayment, J. J., and Thomas, G., Rapidly Solidified Amorphous and Crystaline Alloys, (ed. by B.H. Kear et al.), New York, Elsevier, p. 547, 1982.
21. Molian, P. A., J. of Mat. Sci. 20, p.2903, 1985.
22. Nishiyama, Z., in Martensitic Transformation, ed. M. Fine et al., Acad. Press, New York, San Francisco, London, p.281, 1978.
23. Hornbogen, E., Wear, Vol.33, p.251, 1975.
24. Zum Gahr, K. H., Met. Progr. Vol.116, 4, p.46, 1979.
25. Metals Handbook, Vol.3, (ASM), 1973.
26. Bee, J. V., et al., Met. Trans. A, Vol.10A, 9, p.1207, 1979.

Figure Captions

1. Shapes of laser beam (before-a and after focussing-b melted in plexiglass.
2. Schematic illustration of LHT employed in this study.
3. Macrostructure of pins after LHT- a, c and prepared for wear test-b, d.
4. Cross sections of paths of 3Cr steel after LHT1-a, LHT2-b, and LHT3-c, and overlooped paths after LHT1-e, and LHT2-f and g.
5. SEM and TEM-c micrographs showing large grain in the melted/unmelted boundary.
6. Optical microstructure of 3Cr steel after LHT1-a, LHT2-b and LHT3-c.
7. Pseudo-binary sections of Fe/Cr/C[25] and TTT diagrams [26] of 3Cr and 10Cr steels.
8. OM microstructure -a of 10 Cr steel after LHT1 and SEM micrographs showing grain size in marked (a,b,c) areas.
9. Typical compound layer of 3Cr steel after LHT2. SMZ-shallow melted, HAZ-heat affected and TZ-tempered zones.
10. TEM microstructures of 3Cr steel after LHT1. a,b microstructures of melted zone, bright-c and dark-d field image of (022) austenite surrounding dislocated, lath martensite, e-bright and f-dark field image of $(110)_m$ showing microtwinning in martensite.
11. SEM microstructures of 3Cr steel after LHT1. a-DMZ, b-HAZ, c, CHT substrate, (cross section in plane parallel to heated surface).
12. Fracture of 10Cr steel after LHT1. b, c magnificated areas marked in a.
13. Typical spectra obtained from EDX showing differences in Cr, Mn and Fe in cell boundary and cell center. a, b, c,-SEM, d, e-TEM analysis.
14. SEM micrographs showing presence of retained austenite in 10Cr steel in DMZ-a, melted/unmelted boundary-b, HAZ-c and CHT substrate-d.
15. Micrographs (a, B-OM, c-TEM, d-SEM of thin foil) showing presence of delta-ferrite in 10Cr steel after LHT1, (b-showing lower hardness in this area).
16. Variations of R_{wr} and microhardness of 3Cr-a and 10Cr-b steels with scanning velocity and distance from melted surface, tempering temperature-c and comparison of their R_{wr} and R_{wr} of the other CHT steels-d. In Fig. c and d are presented mean values of R_{wr} of 500um LHT surface layer.

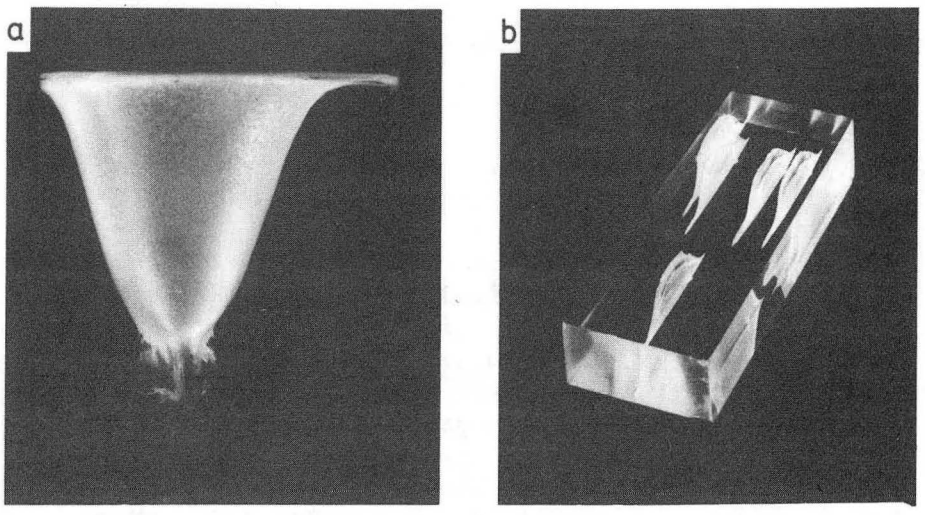

Fig.1

CBB 853-1881A

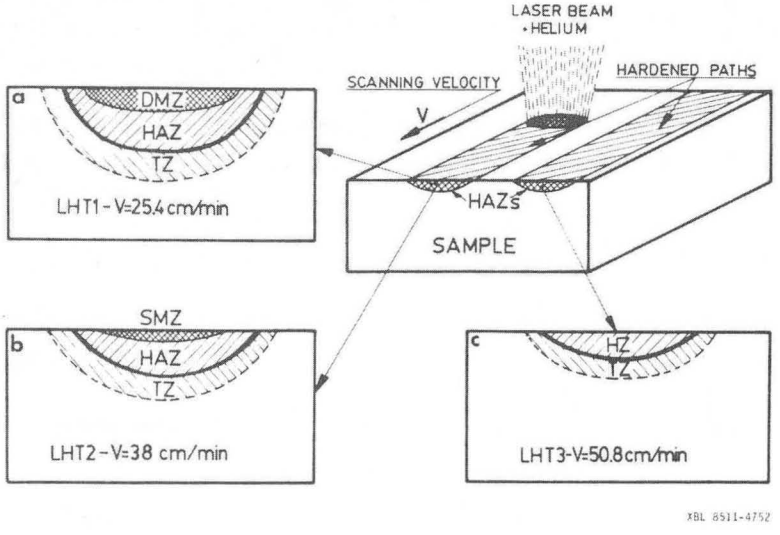

Fig.2

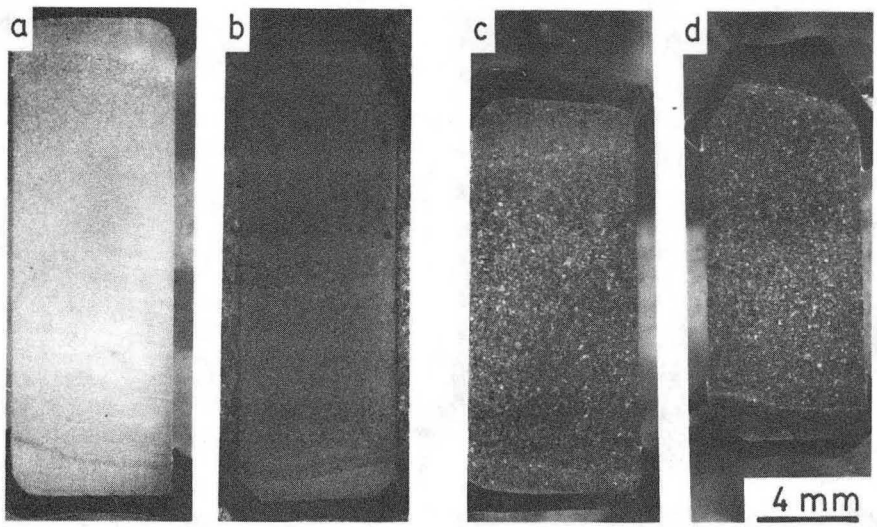

Fig.3.

XBB 862 956

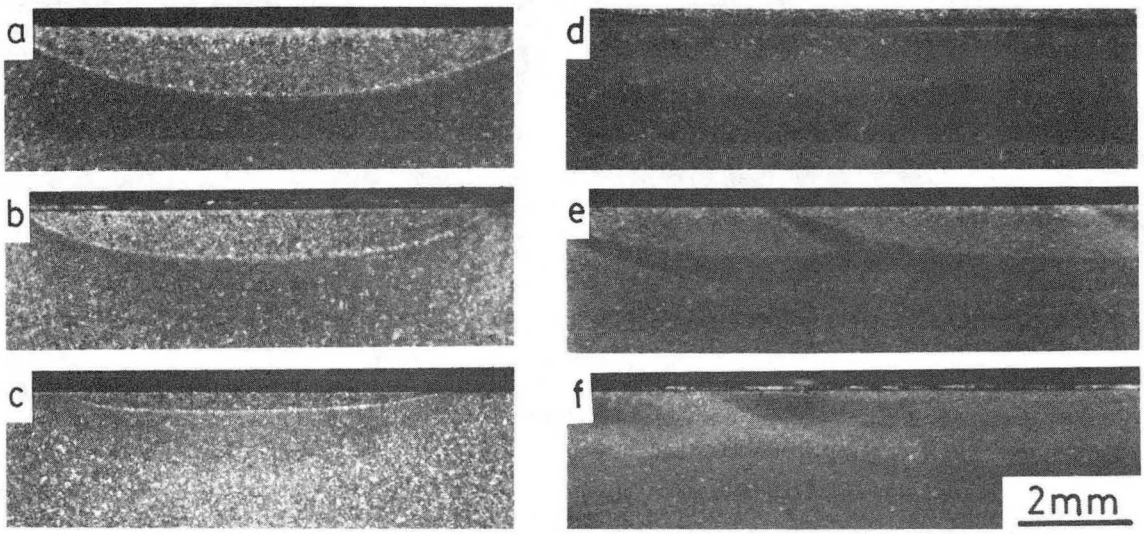

Fig.4.

XBB 863 1985

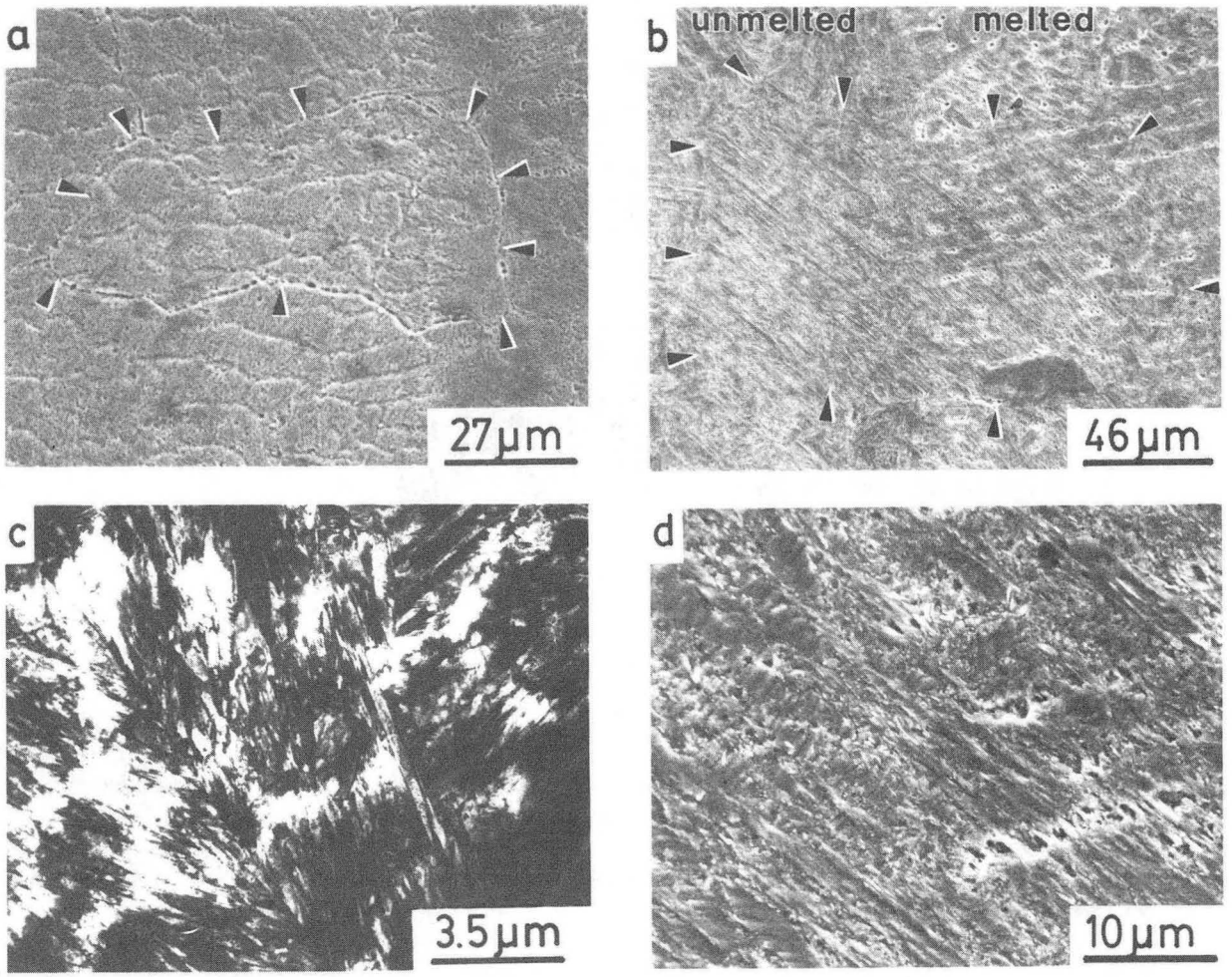

Fig.5

XBB 864-2572

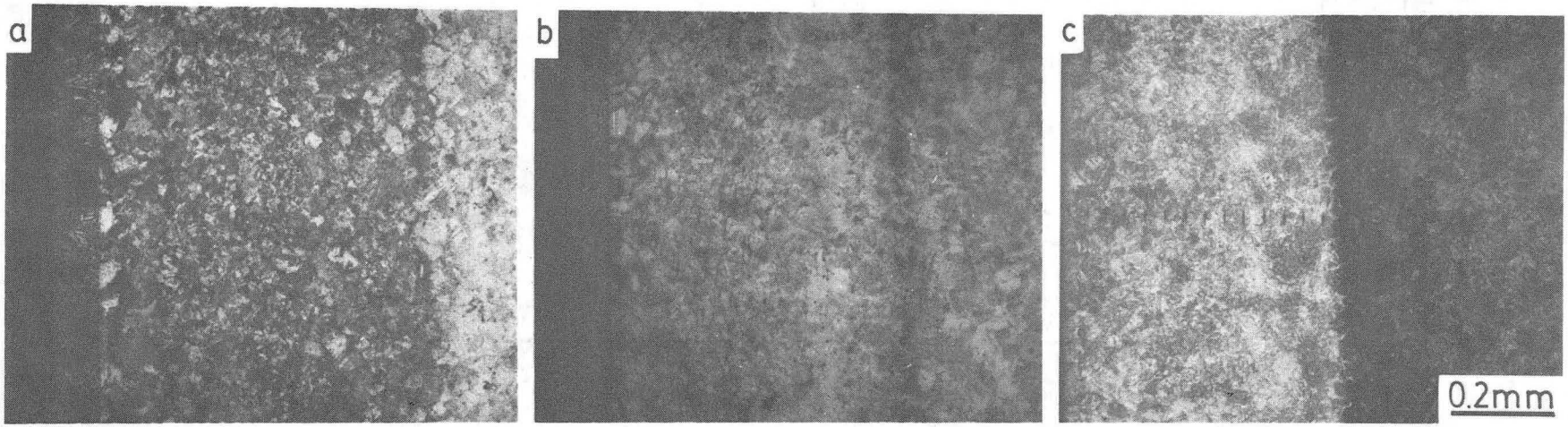

Fig.6.

XBB 863-1983

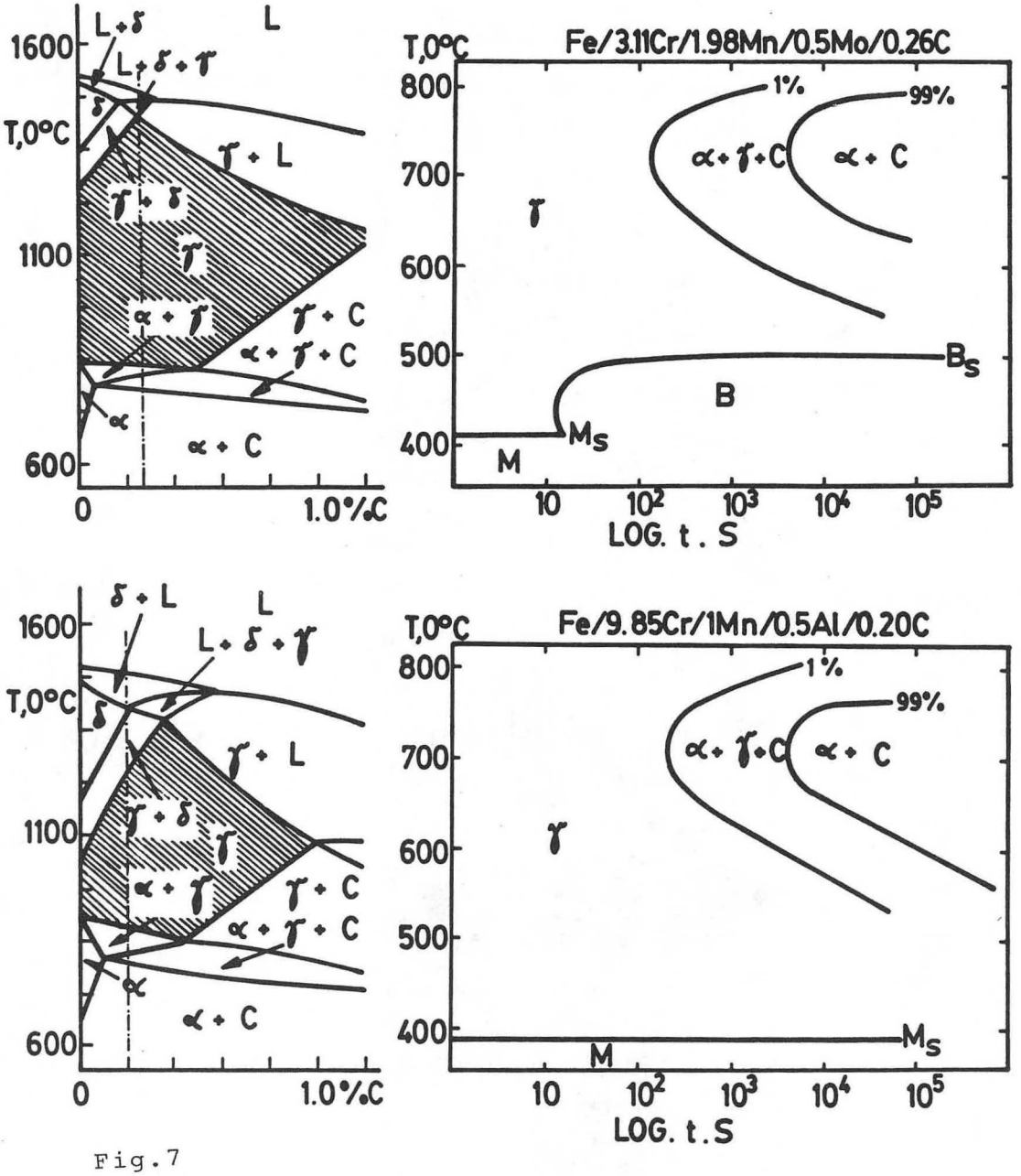

Fig.7

-- XBL 863-1176 -

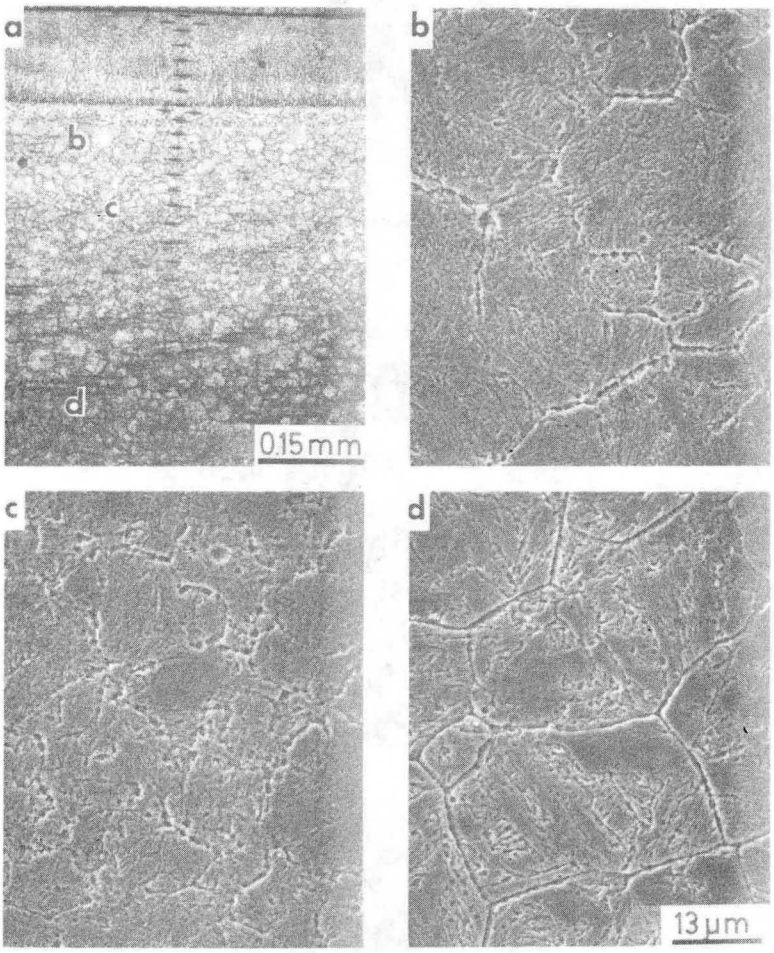

Fig.8

XBB 862-953

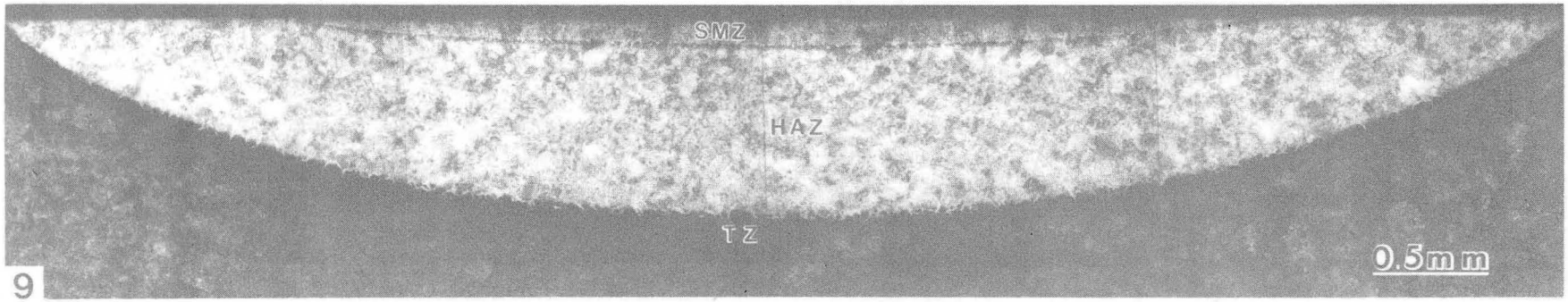

Fig.9

XBB 862-950

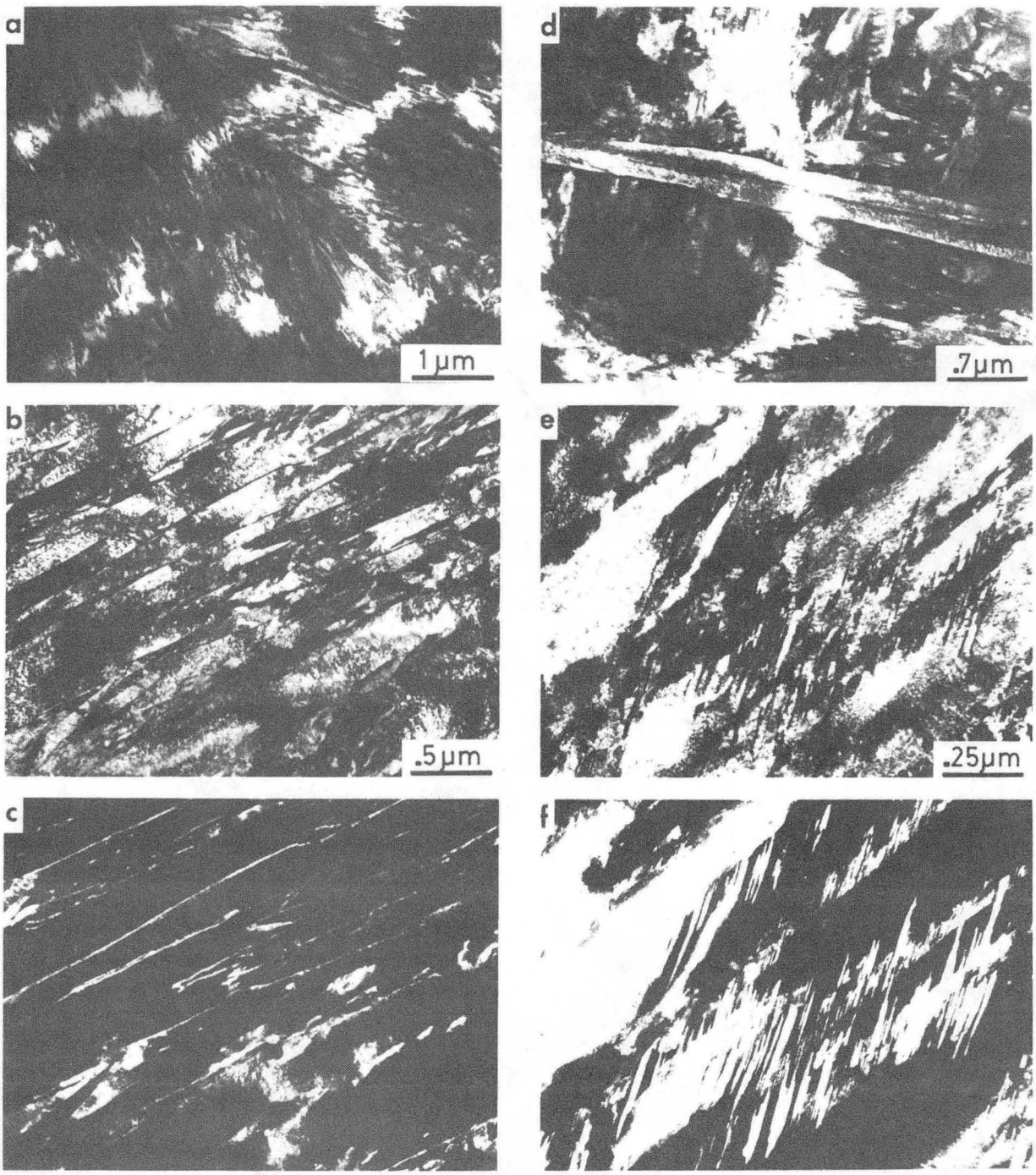

Fig.10

XBB 862-957

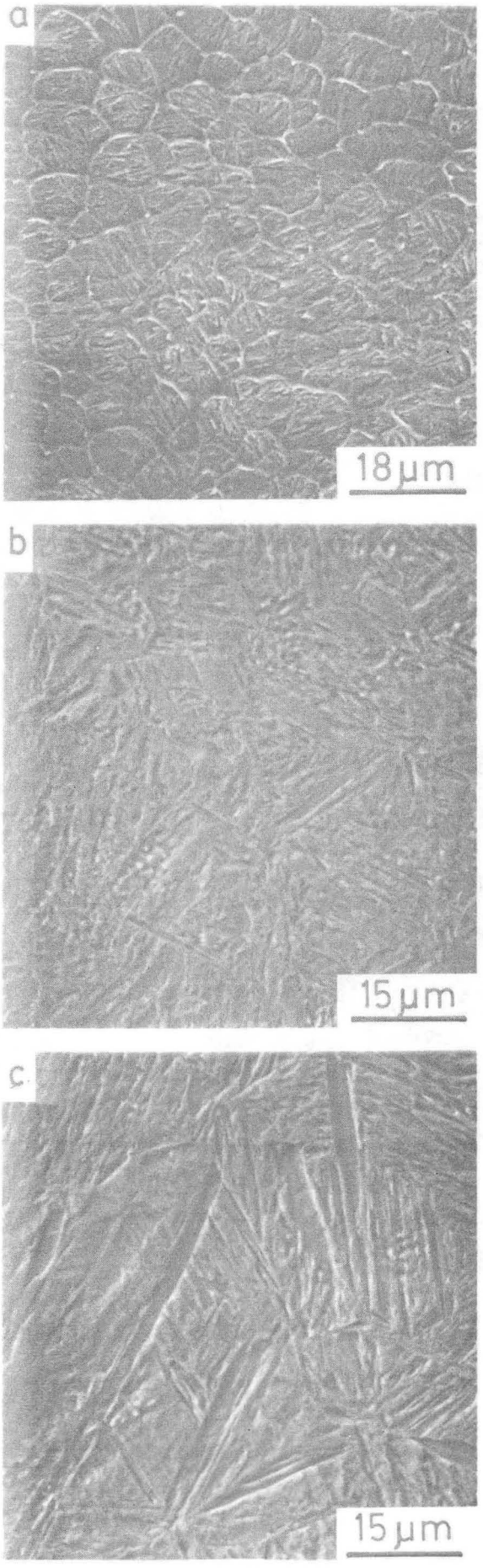

Fig.11

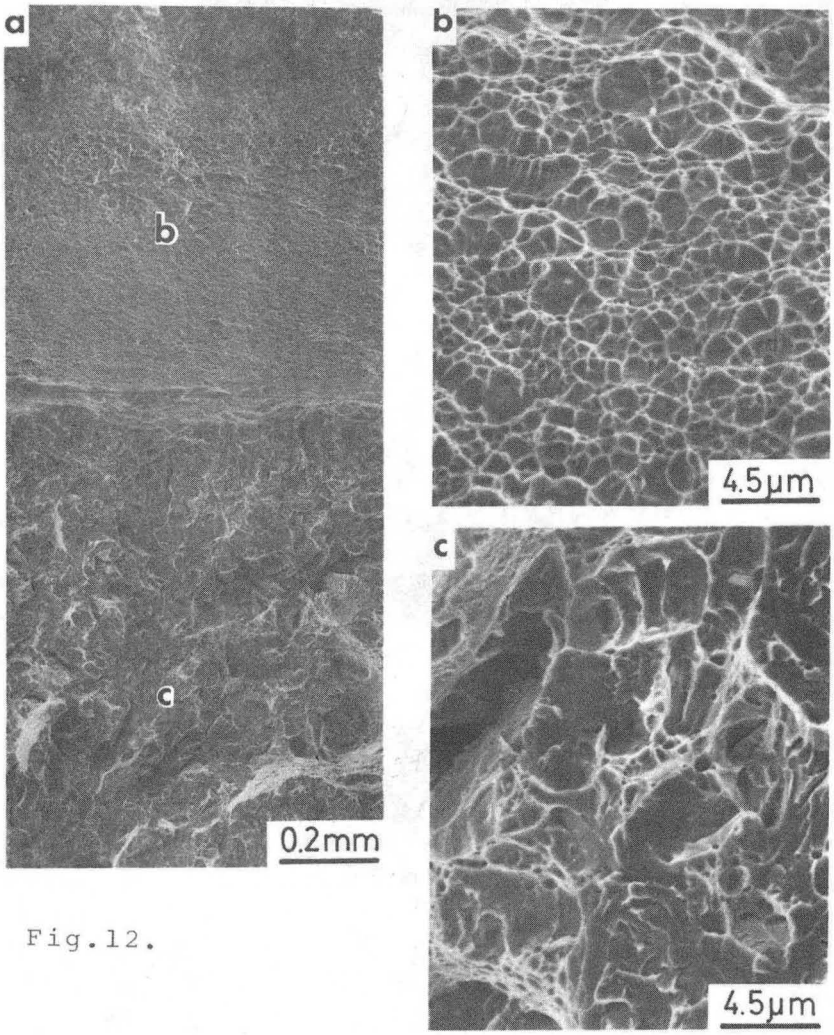

Fig.12.

XBB 862-954

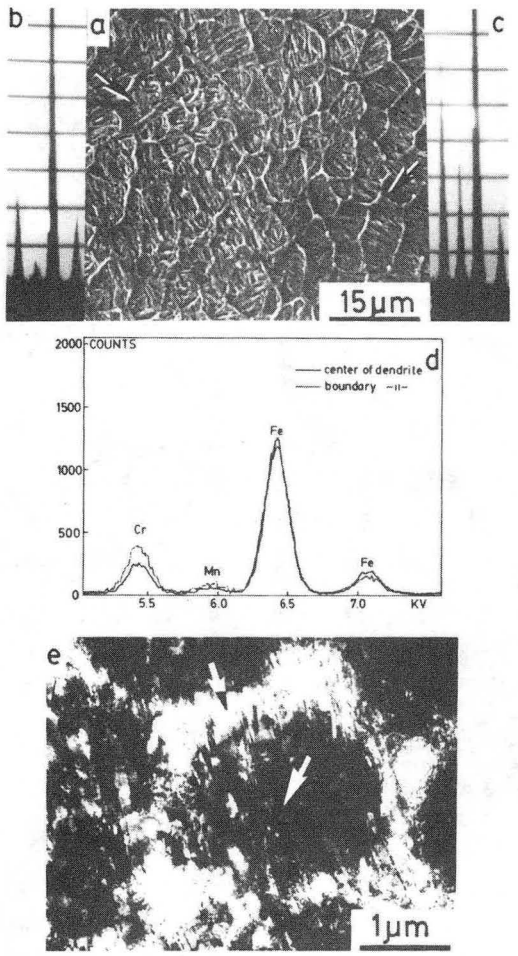

Fig.13. XBB 862-951

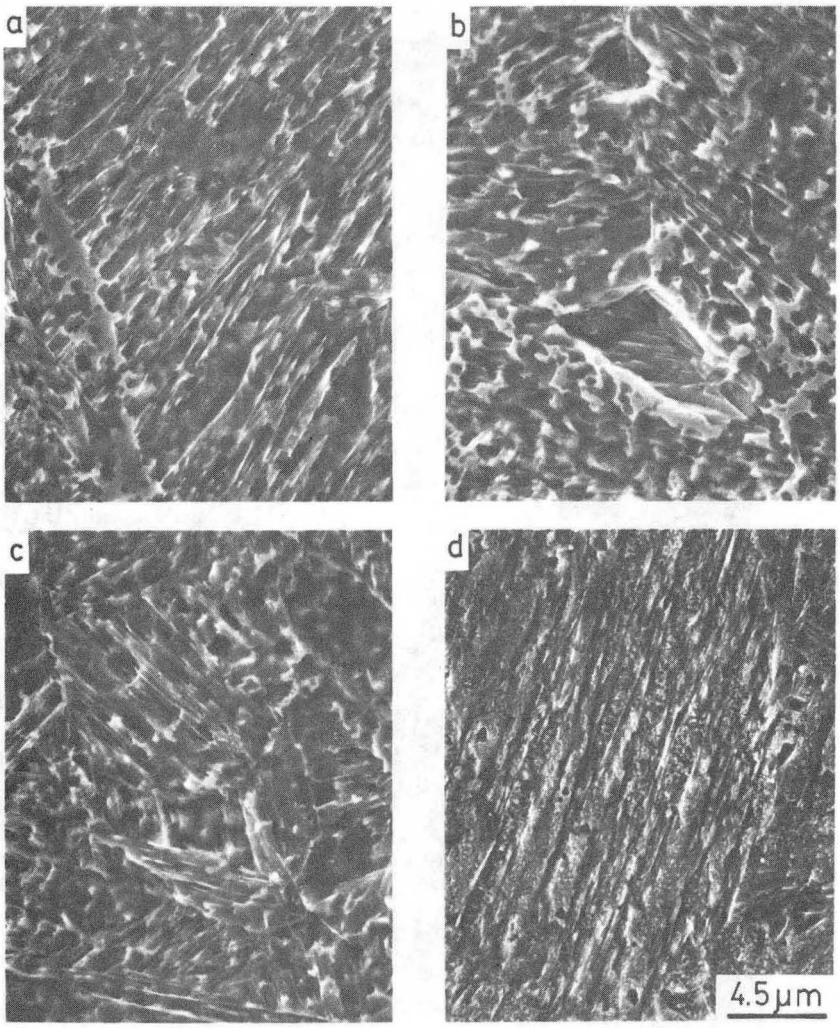

Fig.14.

XBB 863-1992

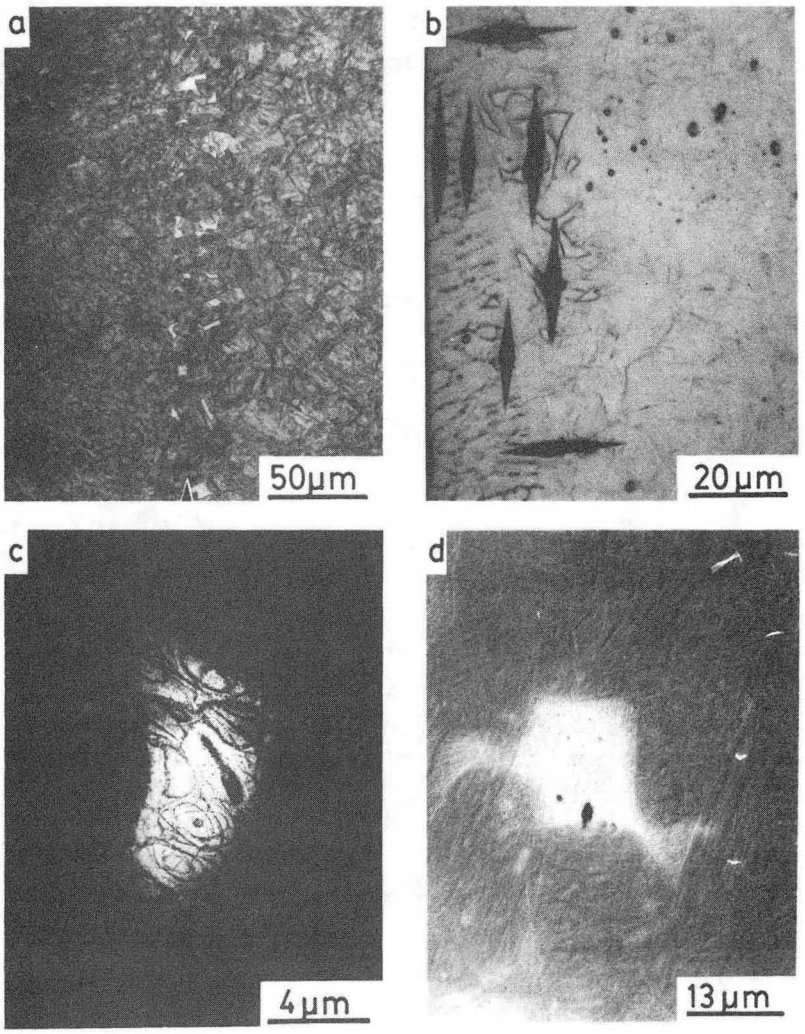

Fig.15.

XBB 863-1991

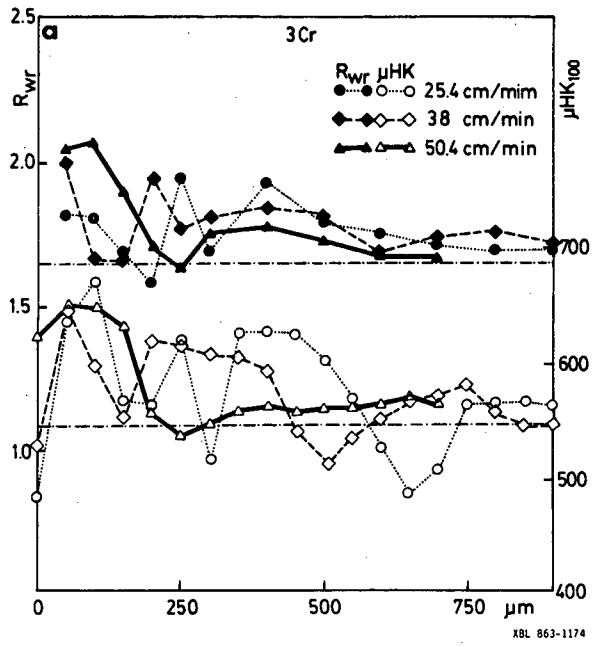
a
3Cr
R_{wr} μHK
25.4 cm/mim
38 cm/min
50.4 cm/min
R_{wr}
μHK_{100}
2.5
2.0
1.5
1.0
700
600
500
400
0
250
500
750 μm
XBL 863-1174

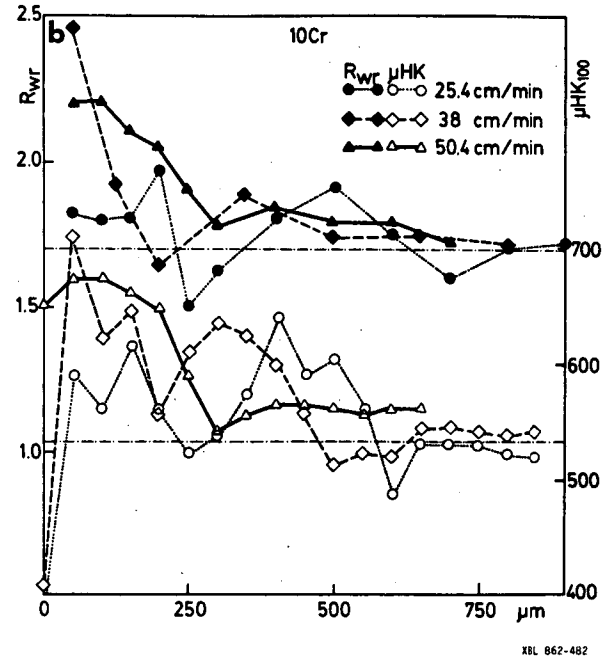
b
10Cr
R_{wr} μHK
25.4 cm/min
38 cm/min
50.4 cm/min
R_{wr}
μHK_{100}
2.5
2.0
1.5
1.0
700
600
500
400
0
250
500
750 μm
XBL 862-482

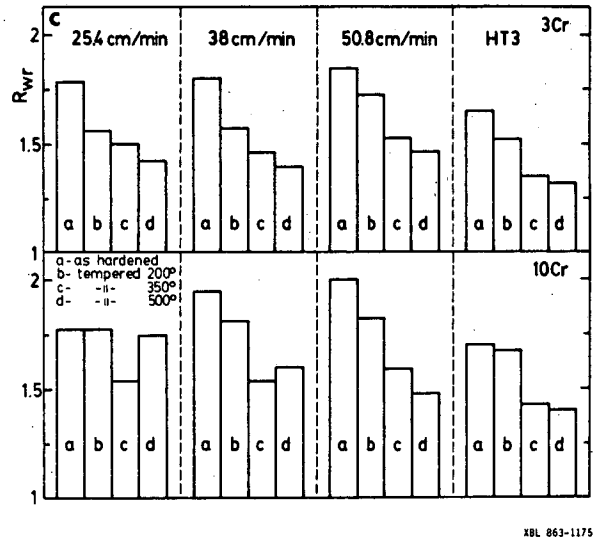
c
25.4 cm/min
38 cm/min
50.8 cm/min
HT3
3Cr
10Cr
R_{wr}
a-as hardened
b- tempered 200°
c- -"- 350°
d- -"- 500°
a b c d
2
1.5
1
XBL 863-1175

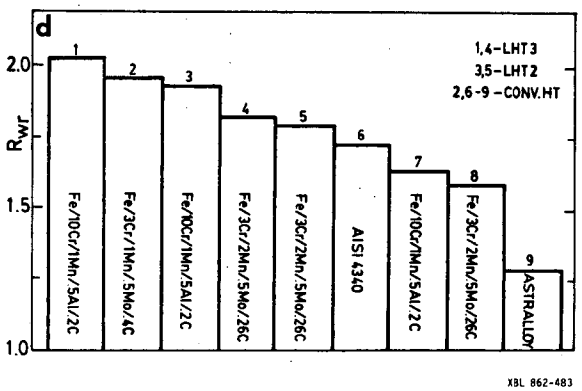
d
1,4-LHT3
3,5-LHT2
2,6-9-CONV.HT
R_{wr}
2.0
1.5
1.0
1
2
3
4
5
6
7
8
9
Fe/10Cr/1Mn/5Al/2C
Fe/3Cr/1Mn/5Mo/4C
Fe/10Cr/1Mn/5Al/2C
Fe/3Cr/2Mn/5Mo/2C
Fe/3Cr/2Mn/5Mo/2C
AISI 4340
Fe/10Cr/1Mn/5Al/2C
Fe/3Cr/2Mn/5Mo/2C
ASTRALLOY
XBL 862-483

Fig.16.

LAWRENCE BERKELEY LABORATORY
TECHNICAL INFORMATION DEPARTMENT
UNIVERSITY OF CALIFORNIA
BERKELEY, CALIFORNIA 94720